Langmuir

Article

pubs.acs.org/Langmuir

Electrokinetic Measurements of Thin Nafion Films

Alexander C. Barbati and Brian J. Kirby*

Sibley School of Mechanical and Aerospace Engineering, Cornell University, Ithaca, New York 14853, United States

Supporting Information

ABSTRACT: We perform an electrokinetic characterization of ~300 nm Nafion films deposited on glass slides over a relatively unexplored region of ionic strength and pH. Owing to the small pore size of the Nafion, we probe the Nafion−fluid interface with the streaming potential measurement, and we probe ionic transport through the entire thickness of the Nafion film with the conductivity measurements. By applying a transport model for each of these measurements, we show that the inferred fixed charge density and characteristic fluid resistance length is different in each case. Analyzing our results with data from the literature, we suggest that our result is consistent with a thin Nafion film that is both nonuniform and weakly hydrated. Our regimen of experimentation and analysis may be generalized to characterize other porous and charged layers.

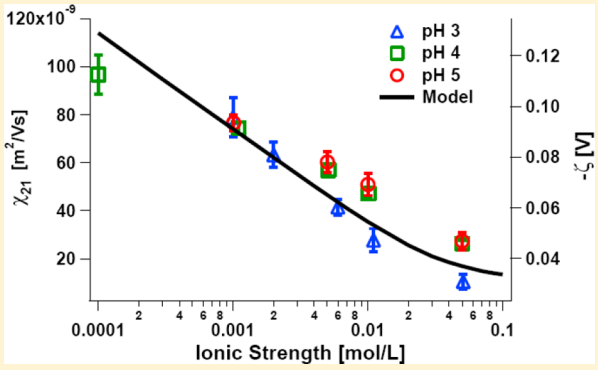

INTRODUCTION

Electrokinetic phenomena, typically characterized by the ζ potential,[1,2] reveal information on the physicochemical state of an interface in contact with an electrolytic solution. Electrokinetic parameters, like the ζ potential, are dependent upon the chemistry of the solid−liquid interface; the pK_a of acidic and basic groups, the ionic nature of the solution,[3] and the presence of surfactants[4] contribute strongly to observed electrokinetic effects. The morphology of the interface is also important; in contrast to a system with charged rigid walls, systems with porous and charged layers can exhibit increased fluxes of mass and current.[5]

The electrokinetic response of a material or system is described by the electrokinetic coupling matrix (EKCM). The EKCM characterizes the response of a system to linear forcing by pressure (∇p) and electrical potential ($\nabla \phi_{ext}$) gradients:

$$\begin{pmatrix} Q/A \\ I/A \end{pmatrix} = \begin{bmatrix} \chi_{11} & \chi_{12} \\ \chi_{21} & \chi_{22} \end{bmatrix} \begin{pmatrix} -\langle \nabla p \rangle \\ -\langle \nabla \phi_{ext} \rangle \end{pmatrix} \quad (1)$$

The angled brackets take the area average of the component of the gradient normal to the channel cross-section, that is, $\langle \nabla \phi_{ext} \rangle = 1/A \int_A \nabla \phi_{ext} \cdot \vec{n}\, dA$. Area-averaged fluxes of volume, Q/A, and current, I/A, are related to the gradients via coupling coefficients: The hydraulic capacitance, χ_{11}, relates the ease with which flow is actuated by pressure, the electrical conductivity, χ_{22}, relates the applied electric field to the driven current, and the off-diagonal terms χ_{12} and χ_{21} communicate the ability of the system to generate flow from an applied potential gradient and current from an applied pressure. These off-diagonal terms are equal by Onsager reciprocity.

Electrokinetic techniques are often used to measure physical and chemical properties of porous and charged layers.[5] Typically, streaming current, streaming potential, and conductivity measurements are coupled with physical measurements of the porous layer and a numerical[6−8] or approximate analytical[6,9−14] models of the transport in the layer. Zimmermann et al.[15] performed a combined analysis to study protein adsorption within a planar electrokinetic cell[16] designed to extract information from streaming current/potential and conductivity measurements. Cordeiro et al.[17] executed a similar set of experiments with the same electrokinetic cell to measure electrokinetic effects with a thermoresponsive polymer layer. In these and other studies, transport models are applied to the collected data to determine charge densities and other physicochemical properties.

Here, we examine a Nafion polymer film in a pseudo-1D configuration. Nafion is important in a variety of industrial applications, most notably as a cation exchange membrane in fuel cells and in electrolytic filtration[18] assemblies. Further, porous polymers are often used as coatings in capillaries to modify the electrokinetic response of the base material,[19] and on electrodes to modify transport properties.[20] In these and other applications, the response of the porous and charged polymer to applied fields, imposed flows, and solutions of different compositions is essential to engineer device performance. In this study, we systematically examine a Nafion thin film deposited on a rigid substrate over a range of pH and salt concentrations using the electrokinetic methods of streaming potential and conductivity. Additionally, we execute X-ray photoelectron spectroscopy (XPS), ellipsometry, and profil-

Received: September 27, 2013
Revised: December 22, 2013
Published: January 30, 2014

   dx.doi.org/10.1021/la403735g | Langmuir 2014, 30, 1985−1993

ometry measurements to further characterize chemical and physical attributes of the Nafion.

In comparison with most materials used in characterization of porous and charged polymer layers,[15,17,21] Nafion is expected to exhibit a larger hydraulic resistance. The generally accepted structure of bulk Nafion consists of a percolation network of aqueous blobs and channels lined with hydrophilic sulfonate groups (as described by the Gierke model[22,23]) interspersed with phases of hydrophobic perfluorinated polymer. Transport occurs in the hydrophilic phase of the material, with a characteristic pore dimension of 1−2 [nm].

We perform streaming potential and conductivity measurements to characterize the electrokinetic behavior of the Nafion−fluid system. Although conductivity measurements are commonly performed on Nafion samples in a variety of electrolytes, these measurements are normally performed in mixtures of [dM] or [M] ionic strength. Our work expands available results in concentration space down to 10 μM for conductivity measurements and 100 μM for streaming potential measurements.

Further, when performing streaming potential measurements, our electrokinetic cell preferentially probes the surface of the Nafion layer. The streaming potential is a result of ions advected by the flow; For a porous material with large mechanical resistance to flow, like Nafion, we expect that pressure-driven flow will actuate a thin region of fluid within Nafion film at the boundary between the porous layer and pure fluid. As the actuated charge is localized to a thin region of the interface, any properties inferred from the measurement may be attributed to this same thin region.

The significance of measuring Nafion both at the interface and throughout the bulk is reinforced by independent interfacial studies of Nafion. Studying the Nafion−air and Nafion−water interface, Bass et al.[24] observed a roughening of the Nafion surface (via AFM) when in contact with water, which they attribute to the reorganization of hydrophobic and hydrophilic polymer. This study[24] further observed a change from hydrophobicity to hydrophilicity of the Nafion surface upon hydration, which was also reported by Goswami et al.[25] At the solid−Nafion boundary, Dura et al.[26] observed multilamellar structures at the interface between Nafion and SiO_2 in hydrated films; these multilamellar structures increase in number and thickness as the humidity is increased. Dura et al.[26] did not observe lamellar structures for similarly prepared films on metal (Au and Pt) surfaces.

Despite their unique ability to infer a localized charge density ρ_f and penetration length λ_0 of the Nafion, electrokinetic studies in a planar configuration have not been pursued to date. Instead, researchers have reported the phenomenological zeta potential or the coupling coefficient χ_{21} in a configuration where the flow proceeds through the Nafion polymer.[27−30] Limited results have been obtained in dispersions of Nafion polymer in a mixture of water and aliphatic alcohols by Zhang et al.;[31] they measured a value of $\zeta^* = -2.807$ ($\zeta^* = F\zeta/RT$, with the thermal voltage $RT/F = 25.7$ [mV] at room temperature) in a solution at pH = 3. Daiko et al.[32] performed layer-by-layer assembly of Nafion and poly(allyamine hydrochloride) and claimed a pH-dependent zeta potential (via laser-light scattering of tracer particles) for Nafion, although direct conclusions about Nafion are obscured by the presence of a second material. Abebe and Farhat[33] performed layer-by-layer assembly of Nafion with various polymers on 0.5 μm particles and claim a pH-dependent charge based upon zeta potential measurements and a color change attributed to dye uptake in the Nafion capping layer; specifically, values of $\zeta^* = -2.203$ at pH = 11 and a value of $\zeta^* = 0$ at $1.2 \leq \text{pH} \leq 1.3$. The porous nature of the material appears to be neglected in these[31−33] electrokinetic analyses of Nafion.

Although many studies report on the conductivity through[27,28,34,34−36] and along[37−41] Nafion membranes, we know of no measurements characterizing the conductivity of Nafion in parallel with an ion-containing fluid. Conductivity measurements have been made with Nafion membranes immersed in liquid, and in controlled atmosphere with varying amounts of humidity.[35,37,38] In nearly all instances, the role of hydration[37−39,42] (often cited as water molecules per charge) along with the diffusivity/mobility[27,35,40,41,43] of the cations has been identified as a controlling factor in the conductivity. Often, the conductivity is expressed[40,44] with an effective mobility of the cationic species, as it may differ from the bulk value. Peckham and Holdcroft[44] provide a review of the structure/morphology properties of ionic conductors, and their relation to the overall conductivity of the material.

This paper is organized as follows. We first describe our electrokinetic cell in detail, and outline the program of measurements, which we perform to characterize the physical and chemical properties of the thin Nafion films. Then, we present results from our streaming potential and conductivity measurements that we interpret using a model[13,14] to predict the charge density and resistive properties of the Nafion film. We then compare these results with available data from other electrokinetic studies on Nafion (performed in different configurations), and propose an explanation for our observed data.

MATERIALS AND METHODS

Sample Preparation. Glass microscope slides (75 mm × 25 mm × 1 mm, VWR) were sonicated for 20 min in mixtures of soap and water, then a 1:1 mixture of methanol and ethanol, rinsed with deionized (DI) water, and dried with N_2. The slides were further cleaned in a solution of 3:1 H_2SO_4/H_2O_2 at 50 °C for 20 min, rinsed several times with DI water, and dried in an N_2 stream.

We coated the cleaned slides with a silane layer to promote adhesion with the Nafion polymer.[45] Following the procedure of Luzinov et al.,[46] slides were immersed in a solution of 1% v/v 3-glycidoxypropyltrimethoxysilane in toluene for 22 h. Care was taken to minimize exposure of the slides to water vapor by performing the silane deposition in a closed container over a desiccant with a gentle N_2 purge. Following immersion, slides were soaked in toluene for 20 min, rinsed in anhydrous ethanol, sonicated in anhydrous ethanol for 20 min, and then dried in a stream of nitrogen gas. After the silane deposition, slides are stored in a closed container over a desiccant and used within 48 h. All solvents used are of ACS Reagent grade.

We implement a solution-casting technique[45,47] with spinning to generate nanometer-thick Nafion polymer layers. A solution of 20% Nafion resin in aliphatic alcohols and water (Sigma-Aldrich No. 663492) was diluted to 3% in 200-proof ethanol. This solution was applied to the silane-treated slides at an area density of 1 mL per 75 mm × 25 mm slide surface and spun at 1000 rpm for 7 s. Following spinning, slides were placed beneath large pyrex Petri dishes on a level surface and cured in a 150 °C oven (air atmosphere) for 1 h. This temperature was selected by the observation that higher curing temperatures lead to more stable films.[47] Following the 1 h cure, the slides were left covered to cool to room temperature on a lab bench. The samples appeared slightly yellowed at the slide edges (i.e., on the edge bead).

Following Nafion deposition and oven curing, we washed the samples in (70%) nitric acid for 1 h at room temperature and then rinsed in DI water and dry in a nitrogen stream. Acid washing ensures

dx.doi.org/10.1021/la403735g | Langmuir 2014, 30, 1985−1993

the Nafion is in proton form (e.g., $-SO_3H$ vs $-SO_3Na$); X-ray photoelectron spectra of the Nafion films after the acid wash do not contain a sodium peak (see the Supporting Information). Additionally, the slight yellowing observed following curing is removed by this acid treatment.

Profilometry Measurements. Mechanical film thickness measurements were performed in wet and dry states. Measurements were performed with a Dektak 6m profilometer (Veeco) and a stylus with a 12 μm diameter tip. The films were mechanically abraded in three positions along the sample centerline, corresponding to upstream, middle, and downstream positions. Four measurements were made at each position. This procedure was performed on a set of three samples at the dry state and each pH and salt concentration condition tested, to characterize the swelling response that we later apply to our electrokinetic samples under similar conditions.

Ellipsometry Measurements. Ellipsometric film thickness and optical property measurements were made on dry Nafion films using a Woollam Spectroscopic Ellipsometer (J. A. Woollam Co., Inc.). Measurements were made on a rectangular silicon substrate with a deposited layer of 1 μm thermal oxide. Processing conditions for Nafion on silicon are identical to films deposited on glass slides, with the amount of 3% resin used adjusted to keep the surface coverage uniform between the two substrates. The silicon surface was used to eliminate backside reflection of the glass substrate. Measurements were taken at incident angles of 65°, 70°, 75°, and 80°, over incident light at wavelengths between 300 and 1000 nm in 5 nm increments (see the Supporting Information for graphical output). Modeling was performed using WVase32 software (J. A. Woollam Co., Inc.).

XPS Measurements. Survey and narrow scans were performed on the Nafion samples to determine atomic composition and bonding information (Surface Science Instrument, SSX-100). A flood gun was used to reduce charging effects on the polymer. All XPS measurements were performed in an evacuated (ultrahigh vacuum) chamber.

Electrode Fabrication. Silver chloride electrodes were prepared using an electrolytic method. Silver wire of 0.5 mm diameter and 5 mm length were installed in Nanoport fittings (IDEX Health and Science) with an ethylene tetrafluoroethylene sleeve. Pairs of silver wire electrodes were anodes in a cell opposite a platinum cathode in a solution of 0.1 [mol/L] HCl, through which a current density of 2 mA/cm^2 is supplied for 30 min. After the deposition, the electrodes are stored with leads shorted in a 0.1 mol/L HCl solution until used.

Experiment Solutions. Sodium chloride solutions (concentrations 1, 5, 10, 50, and 100 mM) were prepared at pH 3, 4, and 5 using hydrochloric acid, sodium chloride salt, and DI water. We measured the pH, temperature, and conductivity of each solution before and after each set of electrokinetic experiments (Mettler Toledo model SevenMulti). Solutions were not purged with inert gas, and the concentrations of bicarbonate and carbonate ions are small as compared to the added ionic species.

Flat Plate Cell and Electrokinetic Measurements. Electrokinetic measurements (streaming potential and conductivity) were performed in a home-built flat plate streaming potential apparatus, similar to designs presented by Van Wagenen and Andrade,[48] and Scales et al.[49] A schematic of this device is presented in Figure 1. A pair of Nafion-coated slides form the channel floor and ceiling separated by a thin (nominally 50 μm) Teflon shim having a cut-out region with length 56 mm and width 9.5 mm. Holes (1/8″ diameter) drilled in the top slide permit access to the channel formed by the Teflon shim. We positioned an instrument pillar above each drilled hole. In addition to establishing a connection to the sample slides, the upstream pillar contains two electrodes (one current sourcing, one voltage sensing), a pressure port, and an inlet port which connects to a syringe pump (KD Scientific). Similarly, the downstream pillar contains a complementary pair of electrodes, and connection to an outlet reservoir. Voltage sensing is performed using a Keithley electrometer (model 6514), current is sourced from a Keithley sourcemeter (model 2400), and pressure is measured using an Omega Engineering 0–5 psi pressure transducer (model PX409). All instruments are connected to a computer and are controlled via (or monitored by) a LabView script.

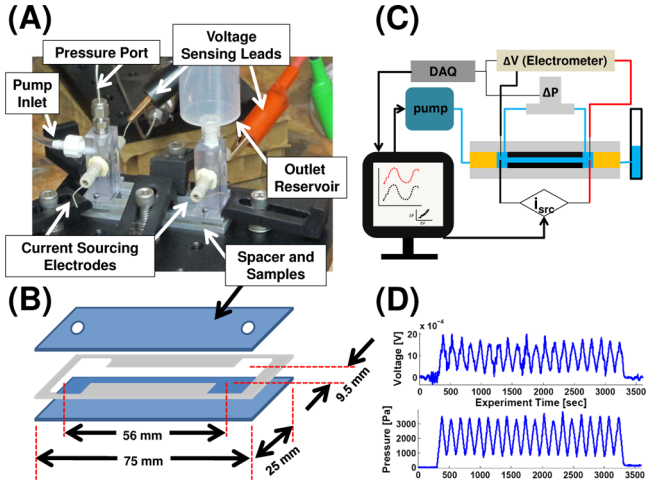

Figure 1. Picture and schematic of the electrokinetic cell with sample data. The assembled cell is shown in (A), with current leads disconnected for clarity, highlighting the various inputs and outputs of the device. The dimensions of the sample slides and shim are shown diagrammatically in (B); the plate separation (cell height, $2h$) is approximately 57 μm. In (C), we present a component-level diagram of the components involved in the streaming potential and conductivity experiments, with sample data from a streaming potential experiment shown in panel (D).

We implement phase-sensitive streaming potential measurements[50] to determine the streaming current coupling coefficient (χ_{21}) of the Nafion–fluid system at each salt concentration and pH. The syringe pump provides a triangular waveform with minimum and maximum flow rates of 0.1 and 0.5 mL/min over a peak-to-peak time of 150 s. The generated pressure and voltage waveforms are collected and dominant peaks from their Fourier transform are used to calculate the streaming potential coupling coefficient:

$$\chi_{21} = -\chi_{22}\frac{\mathcal{F}(\nabla\phi_{ext})}{\mathcal{F}(\nabla p)} \tag{2}$$

Here, χ_{22} is the cell conductivity (measured in our electrokinetic device), and ∇p and $\nabla\phi_{ext}$ are the generated pressure and electrical potential gradients along the direction of flow. The scripted operator, $\mathcal{F}$, denotes the amplitude of the peak (i.e., driving) frequency in each Fourier spectrum.

The cell conductivity is measured with a four-electrode technique to prevent polarization effects.[51] The sourcemeter provides a sequence of currents (maximum 0.1 μA) for 5 s each, and the electrometer measures the potentials required to drive the currents. Ohm's law is used to compute the conductance of the cell, which we convert to a conductivity with knowledge of the cell geometry. The width and length of the cell are measured with a digital caliper, and the cell height is determined from hydraulic resistance measurements.

Samples are repeatedly measured at each combination of pH and salt concentration. Prior to the initial measurement, each pair of Nafion coated slides is soaked in a solution of pH 3, 4, or 5 (0 mM NaCl) for a minimum of four days with the solution exchanged at least once per day. Each pair of slides is examined in a solution containing only HCl followed by analysis in solutions of HCl and 1, 5, 10, 50, and 100 mM NaCl. Experiments at a given pH and salt concentration consist of two streaming potential measurements, four conductance measurements, and one hydraulic resistance measurement. This set of experiments is repeated a minimum of four times at each combination of pH and salt concentration. The first set of experiments at each pH and salt concentration is neglected in our presented data, as these experiments contain a mixture of experiment solutions (e.g., in changing from 1 to 5 mM, a mixture of the two exists in the electrokinetic cell). An average of five sets of experiments are performed on each pair of slides at a given pH and salt concentration,

dx.doi.org/10.1021/la403735g | Langmuir 2014, 30, 1985–1993

and two pairs of slides are used for each pH. Each pair of slides is tested at one pH only. At the end of each experiment, we obtain the streaming current coupling coefficient χ_{21}, the cell conductivity, χ_{22}, the hydraulic conductivity, χ_{11}, as well as the bulk conductivity and pH of the working fluid measured on a separate, benchtop, meter.

RESULTS AND DISCUSSION

Streaming Potential. We present streaming potential data over three decades of pH and NaCl concentration in Figure 2.

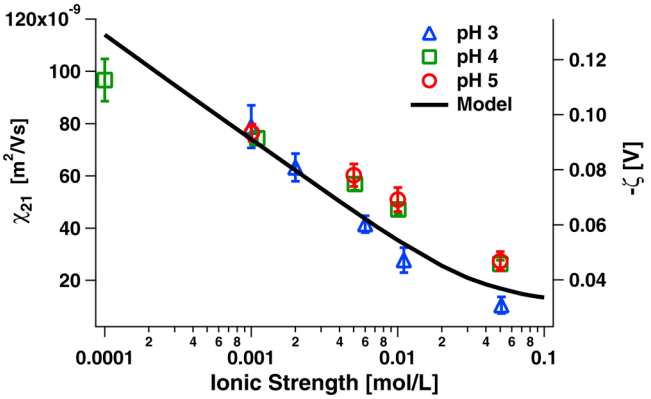

Figure 2. Data and model fit (from eq 5) for χ_{21} and ζ as a function of pH and ionic strength. The model is a function of ionic strength, charge density, and the momentum penetration length λ_0, only.

The streaming current coupling coefficient, χ_{21}, and the phenomenological zeta potential, $\zeta = -\chi_{21}(\eta/\varepsilon\varepsilon_0)$, are plotted as a function of the ionic strength of solution, $I_c = 1/2\Sigma_i z_i^2 c_{i,\infty}$, where z_i and $c_{i,\infty}$ are the valence and bulk concentration, respectively, of the ith component. Additionally, ε_0 and ε are the vacuum permittivity and dielectric constant, assigned values of 8.854×10^{-12} C/V·m and 78, respectively. The fluid dynamic viscosity, η, is 1.003×10^{-3} [Pa·s] at 20 °C.

These data reveal a strong inverse dependence on the logarithm of I_c, and show χ_{21} and ζ to be insensitive to pH. The pH insensitivity is expected based upon the chemistry of the material; Kreuer[22] estimates a pK_a of −6 for the sulfonate groups in Nafion. The scaling of χ_{21} and ζ with the ionic strength of solution is expected based on the Donnan theory of membrane potentials.[52] Inside the membrane, a local balance exists between the charge of the sulfonate groups and mobile cations from solution. This balance predicts a potential difference between the film interior and bulk fluid, which for a symmetric electrolyte with valence z is

$$\phi_D = \frac{RT}{zF}\,\mathrm{arcsinh}\left(\frac{\rho_f}{2FI_c}\right) \tag{3}$$

Here, ϕ_D is the Donnan potential[53] in V, F is Faraday's constant, R is the ideal gas constant, T is the absolute temperature, and ρ_f is the fixed charge density in C/L. This scaling predicts a decrease in the Donnan potential for constant ρ_f and increasing I_c.

The phenomenological ζ potential and Donnan potentials are not equivalent in the Nafion−solution system. The phenomenological ζ potential is the surface potential at the plane of shear,[1,54] and relates to χ_{21} as $\zeta = -\chi_{21}(\eta/\varepsilon\varepsilon_0)$. This relation applies when the separation between surfaces is much larger than the Debye length of the solution ($h \gg \lambda_D$, defined below) and the shear plane and solid boundary coincide. Thus, the phenomenological ζ potential assumes that the surface of polymer is rigid and impermeable; this is inconsistent with our understanding of Nafion as a porous material, and violates eq 3, which requires a fixed charge density and cannot exist in a planar surface. In a previous publication, we derive an approximate form of the coefficient χ_{21} for a porous and charged layer grafted on a rigid surface in a parallel-plate configuration.[13] Our result is written in terms of dimensionless ratios, many of which are known for our thin Nafion films:

$$\begin{aligned}\zeta^* &= \frac{\chi_{21}}{-\frac{\varepsilon\varepsilon_0}{\eta}\frac{RT}{F}} \\ &= -\frac{1}{\beta}\phi_D^* + \left(\frac{\rho_f^*}{\alpha^2\gamma^2} + \phi_D^*\right)\left(1 + \frac{1/\beta - 1}{\cosh(\alpha)} - \frac{\tanh(\alpha)}{\alpha\beta}\right)\end{aligned} \tag{4}$$

Here, $\alpha = \delta/\lambda_0$ parametrizes the hydraulic resistance of Nafion, where δ is the thickness of the Nafion film and λ_0 is the characteristic penetration distance of momentum from the bulk fluid into the Nafion film. The parameter $\beta = h/\delta$ is a dimensionless cell height, with h representing the half-height of the cell (see Figure 1), and $\gamma = \lambda_D/\delta$ compares the thickness of the Debye length, $\lambda_D = [(\varepsilon\varepsilon_0 RT)/(2F^2 I_c)]^{1/2}$ to the thickness of the Nafion film. The remaining terms, $\phi^* = \phi F/RT$ and $\rho_f^* = \rho_f/2FI_c$, are potentials and charge densities made dimensionless by the thermal voltage (for ϕ) and the charge in solution via the ionic strength (for ρ_f).

Very basic information about the Nafion film simplifies eq 4 considerably. Our measurements of the Nafion film thickness, coupled with hydraulic capacitance measurements to characterize the cell height, and reported literature on the small pore size (less than ∼3 [nm]) of the Nafion polymer,[22,23] indicate that α and $\beta \gg 1$. Profilometric film thickness measurements yield an approximate hydrated thickness of 320 nm; with a cell height of $2h = 57$ μm and an a priori estimate of 5 nm for λ_0, $\alpha = 64$ and $\beta = 89$ so we can safely approximate eq 4 as

$$\begin{aligned}\zeta^* &= \frac{\chi_{21}}{-\frac{\varepsilon\varepsilon_0}{\eta}\frac{RT}{F}} \\ &= \phi_D^*\left(1 - \frac{1}{\beta}\right) + \frac{\rho_f^*}{\alpha^2\gamma^2} \\ &= \mathrm{arcsinh}(\rho_f^*)\left(1 - \frac{1}{\beta}\right) + \frac{\rho_f^*}{(\lambda_D/\lambda_0)^2}\end{aligned} \tag{5}$$

The free parameters are ρ_f^* and λ_0; β is known from independent measurements of the film thickness and height of the electrokinetic cell. We fit the parameters λ_0 and ρ_f^* by finding the combination of ρ_f^* and λ_0 that minimize the error between the predicted and experimental values of χ_{21}. During this search process, we restrict ρ_f^* and λ_0 to be identical in each film.

Our model (eq 5) and data (Figure 2) predict a charge density of 0.0582 mol[$-SO_3^-$]/L, which is less than the accepted value of 1.6727 mol[$-SO_3^-$]/L for a 1100 EW Nafion film with a dry density of 1.84 g/cm^3. The fitted penetration length is $\lambda_0 = 1.57$ nm, suggesting that the Nafion film is weakly permeable to fluid flow. The penetration depth is on the same order as the Debye length in solution, and both are much smaller than the thickness of the Nafion film, ∼300 nm. Thus,

dx.doi.org/10.1021/la403735g | Langmuir 2014, 30, 1985−1993

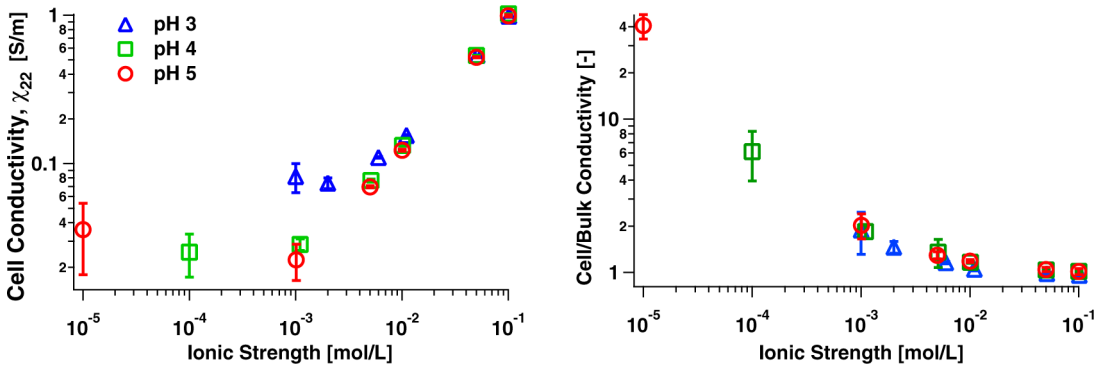

Figure 3. Left: Cell conductivity as a function of solution pH and ionic strength measured using the four-electrode technique. Right: Cell to bulk conductivity ratio. Bulk conductivities are obtained using a commercial conductivity meter in a 50 mL flask, absent surface effects.

the streaming potential measurement constitutes a local probe of the Nafion–fluid interface; free charge a distance $O(\lambda_0)$ into the Nafion is actuated by the flow, with the remaining free charge essentially motionless and neglected in the magnitude of χ_{21}. This value of the penetration length is comparable to the reported pore size based upon the Gierke model of Nafion.[22,23]

Based upon literature descriptions of electroosmotic and Ohmic conductivity through the Nafion polymer, we may anticipate a trend in χ_{21} as a function of pH for solutions of identical ionic strength. Work by Okada et al.[41] describes a dependence of water permeability (average velocity through the membrane per applied pressure) that varies with the type of cationic species in a Nafion membrane. Their data demonstrates that water permeability through the Nafion membrane increases as the proportion of protons in solution. They further show[40,41] that the transference coefficient for water varies in inverse proportion with the concentration of protons in the membrane. The water permeability measure the resistance of flow to pressure, and the transference coefficient indicates the number of water molecules transported by the application of an electric field. Thus, both the mechanical resistance and electroosmotic resistance to flow are expected to change as a function of pH and ionic strength. Based upon the permeability and transference observations of Okada et al.,[40,41] we would expect a trend where solutions with the same ionic strength and different pH are ordered: $\chi_{21}^{pH=3} > \chi_{21}^{pH=4} > \chi_{21}^{pH=5}$. This trend is not observed in our data, suggesting that solution-dependent permeability and transference are minimally present at the Nafion–solution interface, or that these effects are small as compared to other sources of variability in our measurements (e.g., variations from sample to sample). Absence of this trend does not indicate lessened interaction between the fluid and the Nafion film; XPS results (see the Supporting Information) suggest cation exchange by the appearance of a sodium peak in proton-form Nafion films that have been immersed in a solution containing sodium chloride.

Conductivity. We perform conductivity measurements in concert with the streaming potential measurements. The conductivity is a measure of ionic charge transport everywhere within the electrokinetic cell. In contrast to the χ_{21} measurement, in which a pressure-driven flow penetrates a characteristic distance $\lambda_0 \ll \delta$ into the porous layer, the field applied during the conductivity measurements ($\nabla\phi_{ext}$) actuates a body force ($-\rho_e\nabla\phi_{ext}$) on the free charge density (ρ_e) everywhere in the domain. Thus, the conductivity measurements represent the ability of the system to transport ions averaged over the entire domain, in contrast to the local probing of the χ_{21} measurement.

Our conductivity data are presented in Figure 3. We show the conductivity as measured in the electrokinetic cell (the cell conductivity, χ_{22}), and a ratio of cell to bulk conductivities $\sigma_{cell}/\sigma_{bulk}$ as a function of ionic strength and pH. The cell conductivity is an intrinsic measure of the ability of the cell (Nafion and ion-carrying bulk fluid) to transport current; as such, these values are not directly comparable to literature values of Nafion conductivity (presented later).

The observed cell conductivity varies with the pH and ionic strength of solution. These variations reflect differences in the mobilities[55] of the ions H^+, Na^+, and Cl^-. Comparing solutions of the same (or similar) ionic strength but different pH, the solution with lower pH has a larger concentration of high-mobility protons ($\mu_{H+} \approx 7\ \mu_{Na+}$). At larger ionic strengths (by the addition of NaCl), this mobility difference is overcome by increased concentrations of lower-mobility salt ions relative to the protons.

The ratio of the cell to the bulk conductivity indicates that cell effects, owing to the Nafion films, diminish as the ionic strength of the working fluid increases. This trend is expected based upon an equivalent circuit model of the cell conductivity: $\chi_{22} = \sigma_{bulk}(1 - 1/\beta) + 1/\beta\sigma_{Nafion}$ where σ_{bulk} and σ_{Nafion} are the conductivities in the bulk fluid and Nafion, respectively. This relation can be rearranged to yield the conductivity of the thin Nafion film:

$$\sigma_{Nafion} = \sigma_{bulk} + \beta(\chi_{22} - \sigma_{bulk}) \quad (6)$$

The cell conductivity, χ_{22}, includes all conduction mechanisms in the Nafion and fluid portions of the electrokinetic cell. We plot the Nafion conductivity from eq 6 in Figure 4 as a function of ionic strength. These data reveal a relatively uniform conductivity in the Nafion, although the magnitude of the errors preclude definitive conclusions as to the scaling with solution properties. In particular, the 50 and 100 mM data points at pH 5 exhibit a negative conductivity, which is nonphysical. These negative conductivity data points are not considered further in our analysis. Despite this noise, we are able to extract parameters that inform the state of the Nafion film.

We implement a conductivity model[13] to determine the fixed charge density, ρ_f, and penetration length, λ_0, in the Nafion film. Our model incorporates conduction from the bulk, as well as excess Ohmic and electroosmotic conduction in the Nafion layer, $\chi_{22} = \sigma_{bulk} + \sigma_{Ohmic} + \sigma_{EO}$. Like the bulk term, the Ohmic and electroosmotic (EO) subscripted terms account for

dx.doi.org/10.1021/la403735g | Langmuir 2014, 30, 1985–1993

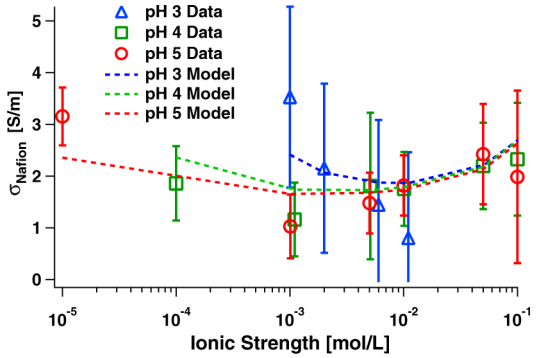

Figure 4. Experimental conductivity data (symbols, as indicated) in the Nafion film with lines from the model presented in eq 10. The error bars represent propagation of standard deviations from the various measurements determining σ_{Nafion}.

conduction effects throughout the domain, not just in the thin Nafion film. We neglect Ohmic and electroosmotic conduction outside of the Nafion film, and validate this simplification by application of the Bikerman[11,56] conductivity formula with inputs derived from our χ_{21} analysis. The estimated contribution from Ohmic and electroosmotic conduction in the bulk fluid is several orders of magnitude lower than the conductivity within the Nafion layer, which validates our simplification. For efficiency, we work in dimensionless conductivities with the scaling $(4/3)FI_c(\varepsilon\varepsilon_0/\eta)\hat{\phi}$. The parameter $\hat{\phi}$ in the conductivity scale is a measure of the mobility of the current-carrying ions (see the Supporting Information for a brief description). We discuss this parameter at length elsewhere.[14]

Our model for the conductivity accounts for conduction in the bulk (driven by the electrophoretic motion of ions) along with Ohmic and electroosmotic excess conductivities within the Nafion film:

$$\chi_{22}^* = \sigma_{\text{bulk}}^* + \sigma_{\text{Ohmic}}^* + \sigma_{\text{EO}}^* \tag{7}$$

$$\sigma_{\text{Ohmic}}^* = \frac{1}{\beta}\sum_i \frac{\phi_i^* z_i}{2\hat{\phi}^*} c_i^* (e^{-z_i\phi_D} - 1) \tag{8}$$

$$\sigma_{\text{EO}}^* = \frac{1}{\beta}\frac{3}{2}\left(1 - \frac{\tanh(\alpha)}{\alpha}\right)\frac{\rho_f^{*2}}{\alpha^2\gamma^2\hat{\phi}^*} \tag{9}$$

Here, ϕ_i^* is the ionic potential of the ith species, z_i is the valence, $c_i^* = c_i/I_c$ is the bulk concentration normalized by the ionic strength, and the remaining symbols have the same meaning as in eq 5. Manipulating eqs 8 and 9 to predict the Nafion conductivity is straightforward. We combine eqs 6 and 7 through 9 to yield

$$\sigma_{\text{Nafion}}^* = \sigma_{\text{bulk}}^* + \frac{3}{2}\left(1 - \frac{\tanh(\alpha)}{\alpha}\right)\frac{\rho_f^{*2}}{\alpha^2\gamma^2\hat{\phi}^*} + \sum_i \frac{\phi_i^* z_i}{2\hat{\phi}^*} c_i^* (e^{-z_i\phi_D} - 1) \tag{10}$$

This result depends only upon the parameters α, γ, ρ_f^*, and the ionic potentials ϕ_i^* which may be calculated[14] from values in the literature for a variety of electrolytes, including ions within Nafion film.[41]

We apply eq 10 to our conduction data, and perform a regression analysis to determine the values of λ_0 and ρ_f, which are the only free parameters. The domains of the parameter space are defined by $10^{-10} \le \rho_f/\rho_f^{(1100\text{EW})} \le 1$ and $10^{-10} \le \lambda_0 \le 10^{-8}$ m, where $\rho_f^{(1100\text{EW})}$ is the charge density of a 1100 EW Nafion membrane. A family of ρ_f and λ_0 pairs yield extrema *within* the domain that minimize the error between the model and experimental data; a single point on the boundary of the parameter space gives a global minimum. This is in contrast to the regression performed on χ_{21}, which gave a unique minimum on the interior of the $\rho_f - \lambda_0$ space. Neither the family of ρ_f and λ_0 pairs nor the minimum on the domain boundary intersect with the minimum identified in the χ_{21} analysis.

Nafion film properties, from the boundary extremum, yield a charge density of 1.6727 mol[$-SO_3^-$]/L and a penetration length $\lambda_0 = 2.58 \times 10^{-10}$ m. The match between the data and experiment is shown in Figure 4. The theory and data agree reasonably well, when the errors in the measurement are taken into account. In extracting the parameters ρ_f and λ_0 from the boundary extremum, we assume that the average charge density in the Nafion thin film is equivalent to the charge density for commercial Nafion membranes. This assumption is reasonable, provided there is enough water in the Nafion film for the charged domains to form a well-connected network, which will allow conduction of cations through the film. Our conductivity measurements are within the range of values obtained for Nafion immersed in water with multiple cations, although our measurements are made in a range of ionic strength that has not been extensively explored. We present a comparison between our data and literature values in Figure 5.

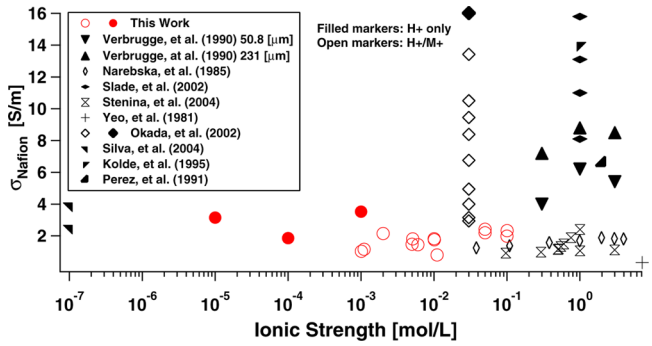

Figure 5. Comparison of conductivities measured in Nafion membranes as a function of ionic strength, with the nature of the electrolyte indicated in the marker type. Shown are the data of Slade et al.,[34] Verbrugge and Hill[36] (for two thicknesses), Kolde et al. (from Slade[34]), Perez et al. (from Slade[34]), Okada et al.,[40] Yeo et al.,[57] Stenina et al.,[58] Narebska et al.,[27] and Silva et al.[59]

The compilation of data in Figure 5 illustrates several points about the conductivity available in the literature and the physicochemical nature of Nafion. There is a large spread in these data: even at the same ionic strength, variations are observed for identical or similar materials among researchers. Two reasons are identified in the literature for this spread. First, the cationic composition in the Nafion and solution govern the conductivity by affecting the hydration in the Nafion membrane. This is readily seen in Figure 5 by comparing the filled markers, where protons are the only cations in solution, to data represented by open and wired markers where the protons and univalent alkali metal ions are present in the Nafion membrane and solution (all are Na^+ except for Yeo et al.[57] which is K^+). Although decreased conductivity for mixed cation electrolytes is consistent within each data set presented, there

dx.doi.org/10.1021/la403735g | Langmuir 2014, 30, 1985−1993

are disagreements between data sets, as, for example, between the data of Okada et al.[40,41] and Verbrugge and Hill.[36] Second, the data by Slade et al.[34] and Verbrugge and Hill[36] reveal a dependence on the thickness of the Nafion layer. This is surprising, because the conductivity is an intrinsic transport property, and should not be dependent on material extents. The four conductivity values from the Slade data are proportional to the thickness of the membrane studied; the highest conductivity (15.8 S/m) is observed for a 208 μm membrane, with thinner membranes (161, 111, and 58 μm) exhibiting a monotonic decrease in the conductivity. The two sets of Verbrugge data show a similar trend, although the decrease is not as strong as that in the Slade data. Not all data sets show size-dependent conductivity for varying thickness; Okada et al.[40] studied Nafion membranes of type 115 (125 μm dry) and 117 (175 μm dry) using an HCl/NaCl electrolyte, and observed no appreciable thickness dependence. In the context of our results, this literature survey suggests that we should observe a decrease in the conductivity for mixed cation electrolytes relative to proton-only electrolytes, as well as a decrease in the conductivity for thin Nafion films relative to thick Nafion films. Although there is appreciable scatter in the data found in the literature, these patterns are apparent in Figure 5.

CONCLUSIONS

In this study, we have combined streaming potential and conductivity measurements to analyze thin Nafion films in contact with an electrolyte solution. We explored a relatively untested region of ionic strength, taking these measurements over three decades of pH at six different values of salt concentration. We coupled our measurements with a theory to extract the fixed charge density, ρ_f, and penetration length, λ_0, as predicted by both the streaming potential and conductivity techniques.

Our results are consistent with a Nafion film that is dehydrated and nonuniform along the film thickness δ. The observed χ_{21} data follow from the advection of mobile charge; in the Nafion film, a volume of fluid with thickness on the order of λ_0 is actuated by the flow. Thus, χ_{21} measurements constitute a localized probing of the Nafion−fluid interface. In contrast, our conductivity measurements average transport of free charge over the entire Nafion film. Because of the values derived from these measurements do not coincide, our results suggest that the Nafion film in our experiments is nonuniform. Specifically, our results are consistent with a Nafion film that is poorly hydrated at the interior. Although we do not explore the source of the hydration in detail, the temperature at which we bake the Nafion during film preparation has been correlated with decreased conductivity measurements on nonwetted Nafion films.[38]

Even with this nonuniformity, we underpredict the expected Nafion charge with our streaming potential measurements. The literature[24,25] indicates that the Nafion−air interface is less hydrophilic than the bulk, and conductivity measurements are consistent with a hydrophobic interfacial region for a wetted Nafion film. Following observations of decreasing Nafion conductivity with Nafion membrane thickness, Verbrugge and Hill[36] hypothesized that the interfacial regions of the Nafion film are of higher ionic resistance than the bulk. As increased hydration and increased percolation of aqueous domains in the Nafion drive conduction,[23,42,44,60] higher ionic resistance is consistent with an interface that is more mechanically resistive and less permeable to flow.

Finally, we have applied two commonly used electrokinetic techniques in an uncommon configuration for a widely studied material. This combination of technique and geometry has enabled us to probe an interface in an uncommon way: we have taken direct measures of the Nafion−liquid interface, and our results suggest that this interface behaves differently than may be assumed if the material were identical to the properties of a bulk Nafion film. Further studies using our technique on this interface, varying, for example, the Nafion thickness, type of electrolyte, or environmental variables such as temperature and pressure, are likely to yield enriching results on the Nafion−fluid interface. Although we have identified several follow-on studies to the material studied presently, this approach is not limited to Nafion surfaces, and would be of great utility for any porous material where the surface structure is posited to exhibit a form or function different from its bulk properties.

ASSOCIATED CONTENT

Supporting Information

Additional details and figures for XPS, ellipsometry, and ionic mobilities. This material is available free of charge via the Internet at http://pubs.acs.org/.

AUTHOR INFORMATION

Corresponding Author

*E-mail: bk88@cornell.edu.

Notes

The authors declare no competing financial interest.

ACKNOWLEDGMENTS

The authors thank the Department of Energy (PECASE) for support. A.C.B. acknowledges fellowship support from the NSF Graduate Research Fellowship Program.

REFERENCES

(1) Hunter, R. J. *Zeta Potential in Colloid Science: Principles and Applications*; Academic Press: New York, 1981.

(2) Kirby, B. J.; Hasselbrink, E. F. Zeta Potential of Microfluidic Substrates: 1. Theory, Experimental Techniques, and Effects on Separations. *Electrophoresis* **2004**, *25*, 187−202.

(3) van der Heyden, F. H. J.; Stein, D.; Beteman, K.; Lemay, S. G.; Dekker, C. Charge Inversion at High Ionic Strength Studied by Streaming Currents. *Phys. Rev. Lett.* **2006**, *96*, 224502.

(4) Lucy, C. A.; Underhill, R. S. Characterization of the Cationic Surfactant Induced Reversal of Electroosmotic Flow in Capillary Electrophoresis. *Anal. Chem.* **1996**, *68*, 300−305.

(5) Barbati, A. C.; Kirby, B. J. Soft Diffuse Interfaces in Electrokinetics - Theory and Experiment for Transport in Charged Diffuse Layers. *Soft Matter* **2012**, *8*, 10598−10613.

(6) Donath, E.; Voigt, A. Streaming Current and Streaming Potential on Structured Surfaces. *J. Colloid Interface Sci.* **1986**, *109*, 122−139.

(7) Ohshima, H.; Kondo, T. Electrokinetic Flow between Two Parallel Plates with Surface Charge Layers: Electro-osmosis and Streaming Potential. *J. Colloid Interface Sci.* **1990**, *135*, 443−448.

(8) Duval, J. F. L. Electrokinetics of Diffuse Soft Interfaces. 2. Analysis Based on the Nonlinear Poisson-Boltzmann Equation. *Langmuir* **2005**, *21*, 3247−3258.

(9) Keh, H. J.; Liu, Y. C. Electrokinetic Flow in a Circular Capillary with a Surface Charge Layer. *J. Colloid Interface Sci.* **1995**, *172*, 222−229.

(10) Duval, J. F. L.; van Leeuwen, H. P. Electrokinetics of Diffuse Soft Interfaces. 1. Limit of Low Donnan Potentials. *Langmuir* **2004**, *20*, 10324−10336.

(11) Dukhin, S. S.; Zimmermann, R.; Werner, C. Intrinsic Charge and Donnan Potentials of Grafted Polyelectrolyte Layers Determined by Surface Conductivity Data. *J. Colloid Interface Sci.* **2004**, *274*, 309−318.
(12) Dukhin, S. S.; Zimmermann, R.; Werner, C. Electrokinetic Phenomena at Grafted Polyelectrolyte Layers. *J. Colloid Interface Sci.* **2005**, *286*, 761−773.
(13) Barbati, A. C.; Kirby, B. J. Force and Flux Relations for Flows of Ionic Solutions between Parallel Plates with Porous and Charged Layers. *Phys. Rev. E* **2013**, *88*, 042408.
(14) Barbati, A. C.; Kirby, B. J. Surface Conductivity in Electrokinetic Systems with Porous and Charged Layers. Submitted, **2013**.
(15) Zimmermann, R.; Osaki, T.; Gauglitz, G.; Werner, C. Combined Microslit Electrokinetic Measurements and Reflectometric Interference Spectroscopy to Study Protein Adsorption Processes. *Biointerphases* **2007**, *2*, 159−164.
(16) Werner, C.; Korber, H.; Zimmermann, R.; Dukhin, S.; Jacobasch, H.-J. Extended Electrokinetic Characterization of Flat Solid Surfaces. *J. Colloid Interface Sci.* **1998**, *208*, 329−346.
(17) Cordeiro, A. L.; Zimmermann, R.; Gramm, S.; Nitschke, M.; Janke, A.; Schafer, N.; Grundke, K.; Werner, C. Temperature Dependent Physicochemical Properties of Poly(*N*-isopropylacrylamide-*co*-*N*-(1-phenylethyl)acrylamide) Thin Films. *Soft Matter* **2009**, *5*, 1367−1377.
(18) Probstein, R. F. *Physicochemical Hydrodynamics*; John Wiley: New York, 2003.
(19) Danger, G.; Ramonda, M.; Cottet, H. Control of the EOF in CE Using Polyelectrolytes of Different Charge Densities. *Electrophoresis* **2007**, *28*, 925−931.
(20) Murray, R. W. Polymer Modification of Electrodes. *Annu. Rev. Mater. Sci.* **1984**, *14*, 145−169.
(21) Yezek, L. Bulk Conductivity of Soft Surface Layers: Experimental Measurement and Electrokinetic Implications. *Langmuir* **2005**, *21*, 10054−10060.
(22) Kreuer, K. D. On the Development of Proton Conducting Polymer Membranes for Hydrogen and Methanol Fuel Cells. *J. Membr. Sci.* **2001**, *185*, 29−39.
(23) Mauritz, K. A.; Moore, R. B. State of Understanding of Nafion. *Chem. Rev.* **2004**, *104*, 4535−4585.
(24) Bass, M.; Berman, A.; Singh, A.; Konovalov, O.; Freger, V. Surface Structure of Nafion in Vapor and Liquid. *J. Phys Chem. B* **2010**, *114*, 3784−3790.
(25) Goswami, S.; Klaus, S.; Benziger, J. Wetting and Absorption of Water Drops on Nafion Films. *Langmuir* **2008**, *24*, 8627−8633.
(26) Dura, J. A.; Murthi, V. S.; Hartman, M.; Satija, S. K.; Majkrzak, C. F. Multilamellar Interface Structures in Nafion. *Macromolecules* **2009**, *42*, 4769−4774.
(27) Narebska, A.; Koter, S.; Kujawski, W. Ions and Water Transport Across Charged Nafion Membranes. Irreversible Thermodynamics Approach. *Desalination* **1984**, *51*, 3−17.
(28) Narebska, A.; Koter, S.; Kujawski, W. Irreversible Thermodynamics of Transport Across Charged Membranes. Part I - Macroscopic Resistance Coefficients for a System with Nafion 120 Membrane. *J. Membr. Sci.* **1985**, *25*, 153−170.
(29) Sicbona, G.; Botre, C.; Botre, F.; Gavelli, G. Electrokinetic Effects Across Nafion 120 Membranes. *Electrochim. Acta* **1991**, *36*, 139−141.
(30) Fabiani, C.; Scibona, G.; Scuppa, B. Correlations Between Electroomotic Coefficients and Hydraulic Permeability in Nafion Membranes. *J. Membr. Sci.* **1983**, *115*, 51−61.
(31) Zhang, H.; Pan, J.; He, X.; Pan, M. Zeta Potential of Nafion Molecules in Isopropanol-Water Mixture Solvent. *J. Appl. Polym. Sci.* **2007**, *107*, 3306−3309.
(32) Daiko, Y.; Katagiri, K.; Matsuda, A. Proton Conduction in Thickness-Controlled Ultrathin Polycation/Nafion Multilayers Prepared via Layer-by-Layer Assembly. *Chem. Mater.* **2008**, *20*, 6405−6409.
(33) Abebe, D. G.; Farhat, T. R. Self-Assembly of Nafion/Poly(vinyl alcohol) at pH = 1.2 and Nafion/Poly(ally amine) at pH = 11. *Soft Matter* **2010**, *6*, 1325−1335.
(34) Slade, S.; Campbell, S. A.; Ralph, T. R.; Walsh, F. C. Ionic Conductivity of an Extruded Nafion 1100 EW Series of Membranes. *J. Electrochem. Soc.* **2002**, *149*, A1556−A1564.
(35) Zawodzinski, T. A.; Derouin, C.; Radzinski, S.; Sherman, R. J.; Smith, V. T.; Sprinter, T. E.; Gottesfeld, S. Water Uptake by Tranport through Nafion 117 Membranes. *J. Electrochem. Soc.* **1993**, *149*, 1041−1047.
(36) Verbrugge, M. W.; Hill, R. F. Analysis of Promising Perflurosulfonic Acid Membranes for Fuel-Cell Electrolytes. *J. Electrochem. Soc.* **1990**, *137*, 3770−3777.
(37) Sumner, J. J.; Creager, S. E.; Ma, J. J.; DesMarteau, D. D. Proton Conductivity in nafion 117 and in a Novel Bis[(perfluoroalkyl)-sulfonly]imide Ionomer Membrane. *J. Electrochem. Soc.* **1998**, *145*, 107−110.
(38) Sone, Y.; Ikdunge, P.; Simonsson, D. Proton Conductivity of Nafion 117 as Measured by a Four-Electrode AC Impedance Method. *J. Electrochem. Soc.* **1996**, *143*, 1254−1259.
(39) Zawodzinski, T. A.; Neeman, M.; Sillerud, L. O.; Gossesfeld, S. Determination of Water Diffusions Coefficients in Perfluorosulfonate Ionomeric Membranes. *J. Phys. Chem.* **1991**, *95*, 6040−6044.
(40) Okada, T.; Moller-Holst, S.; Gorseth, O.; Kjelstrup, S. Transport and Equilibrium Properties of Nafion Membranes with H+ and Na+ Ions. *J. Electroanal. Chem.* **1998**, *442*, 137−145.
(41) Okada, T.; Satou, H.; Okuno, M.; Yuasa, M. Ion and Water Transport Characteristics of Perflurorosulfonated Ionomer Membranes with H+ and Alkali Metal Cations. *J. Phys. Chem. B* **2002**, *106*, 1267−1273.
(42) Hsu, W. Y.; Gierke, T. D. Ion Transport and Clustering in Nafion Perfluorinated Membranes. *J. Membr. Sci.* **1983**, *13*, 307−326.
(43) Goswami, A.; Acharya, A.; Pandey, A. K. Setudy of Self-Diffusion in Monovalent and Divalent Cations in Nafion-117 Ion-Exchage Membrane. *J. Phys. Chem. B* **2001**, *105*, 9196−9201.
(44) Peckham, T. J.; Holdcroft, S. Structure-Morphology-Property Relationships of Non-Perfluorinated Proton-Conducting Membranes. *Adv. Mater.* **2010**, *22*, 4667−4690.
(45) Szentirmay, M. N.; Campbell, L. F.; Martin, C. R. Silane Coupling Agens for Attaching Nafion to Glass and Silica. *Anal. Chem.* **1986**, *58*, 661−662.
(46) Luzinov, I.; Julthongpiput, D.; Liebmann-Vinson, A.; Cregger, T.; Foster, M. D.; Tsukruk, V. V. Epoxy-Terminated Self-Assembled Monolayers: Molecular Glues for Polymer Layers. *Langmuir* **2000**, *16*, 504−516.
(47) Moore, R. B.; Martin, C. R. Chemical and Morphological Properties of Solution-Cast Perfluorosulfonate Ionomers. *Macromolecules* **1988**, *21*, 1334−1339.
(48) Wagenen, R. V.; Andrade, J. Flat Plate Streaming Potential Investigations: Hydrodynamics and Electrokinetic Equivalency. *J. Colloid Interface Sci.* **1980**, *76*, 305−314.
(49) Scales, P. J.; Grieser, F.; Healy, T. W.; White, L. R.; Chan, D. Y. C. Electrokinetics of the Silica−Solution Interface: A Flat Plate Streaming Potential Study. *Langmuir* **1992**, *8*, 965−974.
(50) Tandon, V.; Bhagavatula, S. K.; Kirby, B. J. Transient Zeta-Potential Measurements in Hydrophobic, TOPAS Microfluidic Substrates. *Electrophoresis* **2009**, *30*, 2656−2667.
(51) Schwan, H. P.; Ferris, C. D. Four-Electrode Null Techniques for Impedence Measurement with High Resolution. *Rev. Sci. Instrum.* **1968**, *39*, 481−485.
(52) Teorell, T. In *Transport Processes and Electrical Phenomena in Ionic Membranes*; Butler, J. A. V., Randall, J. T., Eds.; Progress in Biophysics and Biophysical Chemistry; Pergamon Press: Oxford, 1953; Vol. 3, Chapter 9, pp 305−369.
(53) Davies, J. T.; Rideal, E. K. *Interfacial Phenomena*; Academic Press: New York, 1963.
(54) Kirby, B. J. *Micro- and Nanoscale Fluid Mechanics Transport in Microfluidic Devices*; Cambridge University Press: Cambridge, 2010.

(55) Bard, A. J.; Faulkner, L. R. *Electrochemical Methods - Fundamentals and Applications*; Wiley: New York, 2001.
(56) Lyklema, J. *Fundamentals of Interface and Colloid Science: Vol. II Solid-Liquid Interfaces*; Elsevier: Amsterdam, 1995.
(57) Yeo, R. S.; Chan, S. F.; Lee, J. Swelling Behavior of Nafion and Radiation-Grafted Cation Exchange Membranes. *J. Membr. Sci.* **1981**, *9*, 273−283.
(58) Stenina, I. A.; Sistat, P.; Rebrov, A. I.; Pourcelly, G.; Yaroslavtsev, A. B. Ion Mobility in Nafion-117 Membranes. *Desalination* **2004**, *170*, 49−57.
(59) Silva, R. F.; De Francesco, M.; Pozio, A. Solution-Cast Nafion Ionomer Membranes: Preparation and Characterization. *Electrochim. Acta* **2004**, *49*, 3211−3219.
(60) Hickner, M. A. Water-Mediated Transport in Ion-Containing Polymers. *J. Polym. Sci., Part B: Polym. Phys.* **2012**, *50*, 9−20.